

**ULTRASONIC TECHNIQUES FOR REPAIR OF AIRCRAFT STRUCTURES WITH
BONDED COMPOSITE PATCHES**

S.H. Smith
N. Senapati
R.B. Francini

113070

Battelle
505 King Avenue
Columbus, Ohio

SUMMARY

This is a paper on a research and development project to demonstrate a novel ultrasonic process for the field application of boron/epoxy (B/E_p) patches for repair of aircraft structures. The first phase of the project was on process optimization and testing to develop the most practical ultrasonic processing techniques. Accelerated testing and aging behavior of precured B/E_p patches, which were ultrasonically bonded to simulated B-52 wing panel assemblies, were performed by conducting flight-by-flight spectrum loading fatigue tests. The spectrum represented 2340 missions/flights or 30 years of service. The effects of steady-state applied temperature and prior exposure of the B/E_p composite patches were evaluated. Representative experimental results of this phase of the project are presented.

INTRODUCTION

One of the major technical thrust areas in the U.S. Air Force aging aircraft program is the development of structural repair techniques. Primary emphasis is on the development of efficient, durable, inexpensive, and easily implemented repair technology. Previous repair technology has involved the use of metallic structural repair patches and techniques using mechanical and/or bonding techniques [1]. There is an adequate structural material database and design guidelines for designing and installing these aircraft structure repairs. In the past several years, B/E_p composite patches have been used to repair several U.S. Air Force aircraft [2-9]. The thermal blanket curing process was used to install B/E_p composite precured patches. This process takes several hours to cure the adhesive at the required curing temperature not to exceed 250°F.

With U.S. Air Force support, the authors have developed an ultrasonic curing process for the field application of B/E_p composite patches to B-52 aircraft upper wing structures [10]. A summary of the results of this development project is presented in this paper. The project consisted of an initial phase for determining the desirable ultrasonic curing conditions and parameters. Double lap

shear specimens with B/E_p composite strips bonded to 7075-T6 and T651 adherents were tested to determine shear strength and preferred curing conditions. The verification testing of the composite patch design and the ultrasonic curing process consisted of conducting accelerated fatigue and prior exposure tests on repaired structural panel assemblies that simulated the B-52 wing at wing station 402, S-21. Special instrumentation was used to monitor the strain levels in the composite patches and aluminum substrates and to measure the fatigue crack growth behavior during spectrum load testing.

EXPERIMENTAL METHODS AND RESULTS

The experimental techniques and procedures used in this project are described in two parts. The first part is on approaches used in identifying the desired parameters for the ultrasonic bonding process for precured composite patches. The second part involves the experimental techniques and procedures used in the panel assembly testing.

Fabrication of Boron/Epoxy Patches and Test Specimens

The B/E_p patches were precured in an autoclave using a vacuum bag process. All plies in the patches were unidirectional and cured in accordance with the material supplier procedures at a pressure of 50 psi and a temperature of 350°F for 90 minutes. The adhesive selected for bonding the B/E_p patches to the 7075-T6 and T651 aluminum substrates was FM-73 grade 10 and had a polyester mat. The adhesive was stored at 0°F. During room temperature assembly of the specimens any adhesive left over seven days was discarded. The ultrasonic bonding of the B/E_p patches is very sensitive to the surface preparations of the aluminum substrates. Therefore, the surfaces were phosphoric acid anodize and BR127 primed according to procedures defined by the Air Force for field application to B-52 wing structures.

Identification of Process Parameters

The ultrasonic process has several advantages over the thermal blanket technique of curing adhesively bonded composite patches. The advantages are: (1) a better wetting of the substrate surface with the adhesive due to shear thinning with the high intensity ultrasonics, (2) accelerated chemical reactions, (3) less time needed to reach the required curing temperature, (4) a more consistent bond strength, and (5) lower and more uniform residual stresses after cool-down.

The laboratory scale ultrasonic bonding fixture is shown schematically in Figure 1. A series of parametric screening tests were conducted to gain insight into the primary variables and their sensitivity in ultrasonic curing of the B/E_p patches with FM-73 adhesive. It was these variables that were investigated during the parametric screening tests described below. The variables and their ranges investigated were:

Coupling Material—Its purpose was to transfer the ultrasonic energy into the patch. Without a coupling material, very little ultrasonic energy can be transferred to the adhesive via the patch. More than ten types of coupling materials were investigated under this program. The top two were a polymer compound (polyisobutadiene) and a red rubber (styrene butadiene) that was 0.060-inch thick.

Ultrasonic Power—A watt meter was used to measure the power delivered to the ultrasonic converter. The range of powers investigated was 50 to 105 watts. Power levels as high as 400 watts were investigated with the larger size validation test panels.

Duration of the Ultrasonic Energy—During the parametric screening tests the length of time the ultrasonic energy applied to the patch varied from 5 to 120 minutes.

Coupling Pressure—This is the pressure or force that was applied to the patch and test coupon during the application of ultrasonic energy. The force was applied using the hydraulic jack shown in Figure 1. The pressures investigated ranged from 5 to 15 psi.

Several screening tests were conducted to evaluate the thermal cure cycle produced by the ultrasonic bonding technique. Figure 2 shows a plot of temperature versus time for three variable combinations of power, time, and pressure. These are results for five plies of B/E_p bonded to aluminum strips. An embedded thermocouple in the FM-73 adhesive was used to measure temperature with time. As can be seen by the data, a stable temperature is reached after about 15 minutes. Several additional tests were performed with five plies and different combinations of power, time, and pressure. Some screening tests were also conducted with 15 and 40 ply samples. These data were used to select the desired conditions for ultrasonic bonding.

The results of the screening tests were used to develop a master baseline indexed sample for evaluating the degree of cure produced by the ultrasonic process. Figure 3 shows the baseline sample that was developed for undercured, cured, and overcured samples. All subsequent testing and failure mode identification of samples were correlated to this master baseline sample.

The second part of the project involved conducting mechanical tests to quantify the process. In adhesive bonding characterization testing either wedge or lap shear tests are performed to evaluate the integrity of the bondline and process. Double lap shear tests were conducted on ultrasonically cured samples that were bonded according to the desired conditions established in the screening phase. The testing procedures defined in reference 11 were followed. Table 1 shows some of the results for the lap shear strengths developed using the process.

Flight-by-Flight Spectrum Loading Fatigue Tests

Several iterations were performed on the geometry and configuration for the fatigue test specimens. The requirements for the configuration were: (1) that the panel thickness had to be 0.25-inch thick, (2) B/E_p patches were to be bonded to both sides of a single edge crack of 0.30-inch length, (3) grip ends of the specimen had to be designed such that failure would occur in the cracked

section of the panel and not in the grips, and (4) panel configuration and geometry had to be such that monitoring crack growth and load transfer during fatigue could be accommodated.

Initially a single 0.250-inch-thick 7075-T651 aluminum rectangular panel configuration with the B/E_p patches bonded to each surface of the panel with the edge crack was selected. However this configuration was not accepted because of the difficulty and unassured reliability of being able to bond two patches ultrasonically on both sides of the panel at the same time. The second idea of a configuration was to split the thickness of the panel into two 0.125-inch-thick 7075-T6 sheets and ultrasonically bond the two patches on the panels separately and then adhesively bond the two together to form the equivalent 0.250-inch thickness. This configuration had the drawback that Krak gages could not be used on the back side of the crack surface to measure and monitor fatigue crack growth rates. The final idea was to use a honeycomb core or other separator between the two skins/sheets and cut out the core around the crack area for the Krak gages. The honeycomb core or other separator would be adhesively bonded to the aluminum face sheets/skins. This configuration had the added built-in bucking stability required for spectrum loading fatigue testing with compression loading in the spectrum. This concept was retained and the honeycomb core was replaced with Teflon sheets and not bonded to the aluminum face skins/sheets. Solid aluminum inserts were selected as spacers for the grip areas. Figure 4 shows the final specimen configuration selected for the simulated repair. The B/E_p repair patches were eight layers thick with 0.30 and 0.10 inch/ply ramp ups for the vertical and horizontal directions, respectively.

In the grip area, the two repaired sheets were separated by a 7075-T 0.190-inch-thick spacer sheet. The overall geometry of the panel was 8 x 32.5 inches and 6 x 20 inches in the test section. Three 1-inch-radii fillets were machined at the end of the test section. The panel grip ends were designed to accommodate the 50 kip machine grips and bolts with four 17/32-inch- and one 1.00-inch-diameter holes at each end. The panel grip ends and the grips were grit blasted for friction gripping in the grip area. All bolts were torqued to 110 in-lbs.

Instrumentation and Equipment

The flight-by-flight spectrum loading tests conducted on the panel assemblies consisted of four series of tests. These were room temperature, -65°F (-53.9°C), 180°F (82.2°C), and room temperature with prior exposure at 95 percent relative humidity and 180°F (82.2°C) for 60 days. Three fatigue tests were conducted per testing series. The following describes the instrumentation and equipment used for the series of tests.

Figure 5 shows a photograph of the 50 Kip INSTRON electrohydraulic system setup with gripping fixtures and load-control console equipment that was used in the fatigue and residual strength testing of the panels. In addition, this system consisted of the primary data taking equipment, which included a 486 PC computer, Labtech software, and signal conditioning equipment. This system was used to measure and monitor the output of the strain gages, Krak gages, and thermocouples. The output of the Krak gages was read by a FRACTOMAT instrument, consisting of two channels for readout. A strip chart recorder was used to continuously measure the spectrum loading applied to the panel assemblies in each test series.

The spectrum loading fatigue testing of the panels for test series 2 and 3 at -65°F (-53.9°C) and 180°F (82.2°C), respectively, required an environmental chamber around the test panel and the repaired area of the final assembled panel. Figure 5 also shows the environmental chamber and the antibuckling guides used in the fatigue testing. A Lexanl (polycarbonate) chamber was constructed and used for -65°F (-53.9°C) and 180°F (82.2°C) steady-state testing temperature environments. This chamber was designed to serve as an external out-of-plane buckling guide and used in all tests. The chamber was nominally $9 \times 9 \times 2$ inches in volume and contained four longitudinal stiffeners, which were bonded to the Lexanl chamber walls. The stiffeners acted as buckling guides, and Teflon pads were bonded to the bottom surface to ride against the aluminum. The stiffeners were grooved to allow for environmental media circulation. The chamber was sealed with insulation material. The experimental setup for the -65°F (-53.9°C) steady-state temperature testing used liquid nitrogen as the cooling media. The temperature in the environmental chamber was controlled within $\pm 5^{\circ}\text{F}$ and monitored with two probe-type thermocouples. The type of probe thermocouple that was selected was the OMEGA Type K with an exposed junction and 304SS material [12]. The temperatures were applied at a rate of 20°F per minute until the steady-state temperature was reached. The experimental setup for the 180°F (82.2°C) steady-state temperature used hot air and was circulated using a hot air blower. The temperature control and applied rates were the same as for the -65°F (-53.9°C) testing.

The series 1, 2, and 3 were preconditioned according to ASTM D 618 Procedure which was 50 percent R.H. and 73.4°F (23.0°C) for 40 hours [13]. This was performed in an ambient laboratory room. A final series of panels, series 4, were environmentally preconditioned. The composite patches which were bonded to aluminum sheets were preconditioned at 95 percent R.H. and 180°F for 60 days in an environmental preconditioning chamber. The environment was circulating hot and humid air and was monitored and controlled using thermocouples for the dry and wet bulb temperatures. The temperatures were read with a digital readout instrument.

Each of the fatigue panels in the test series was instrumented with Krak gages, strain-gage rosettes, and thermocouples as shown in Figure 4. The criteria in the selection of all of the types of instrumentation were based on the post testing environments of the spectrum loading fatigue combined with the applied steady-state environments of -65°F (-53.9°C) and 180°F (82.2°C).

Type KG-B30 with 30 mm or 1.18-inch effective crack length measurement range was selected for use with an initial edge notch of 0.30 inch or 7.62 mm. [14]. This Krak gage is a foil made of constantan alloy (5 micron or 0.0002-inch thickness) with an epoxy-phenolic glass-fiber-reinforced backing (50 microns or 0.002-inch thickness). The gages were mounted with the crack gage backing exactly flush with the longitudinal edge of the aluminum sheet. The apex of the V-groove of the gage was coincident with the tip of the machined notch. The gages were adhesively bonded to the aluminum surface using TTI 353-ND single-part epoxy adhesive. The procedures of reference 18 were followed. Figure 4 shows the edge view of the mounted Krak gages. The installation of the gages was performed in the laboratory under ambient conditions.

Strain-gage rosettes were used to measure the strain levels in the B/E_p patches and the aluminum sheets. The strain gage data taken from these rosettes was used in monitoring the load transfer behavior from the cracked skin of the aluminum to the B/E_p repair patch. This data was

used as a measure of the effectiveness of the patch in retarding or stopping fatigue crack growth. Figure 4 shows the locations of the strain gage rosettes on the B/E_p patches and the aluminum sheets.

The type of strain-gage rosette selected for the B/E_p composite patches was based on (a) thermally activated coefficient of thermal-expansion compatibility of the gage with the substrate, (b) the post-temperature steady-state temperature environments of -65°F (-53.9°C) to 180°F (82.2°C), and (c) the spectrum loading cyclic fatigue life requirement. Micromeasurements WK-06-062RB-350 (unstacked/uniplanar) 45-degree delta strain-gage rosette and bonded with M Bond 610 adhesive satisfied these criteria. All strain gages were self-temperature-compensating gages and were mounted according to the recommended guidelines of strain-gage applications to composites [15 and 16].

Each of the aluminum skins of the repaired panels was precracked under constant amplitude tension-tension loading with $P_{max} = 22.5$ kips ($S_{max} = 15.0$ ksi), $P_{min} = 0.0$ kips ($S_{min} = 0.0$ ksi), and $R = 0.0$. The cyclic frequency of the loading was 5 Hz. The constant amplitude fatigue loading was applied until the cracks were detected by each of the Krak gages of the panel. The results showed that all of the skin panels were precracked in 1260 to 1272 cycles.

The spectrum loading block was made up of Missions A, B, C, D, E, and F for blocks 1 and 2 and the repeat mix as shown in Table 2 test spectrum. Additional missions as defined for the 10th application of a given mission were incorporated into the building blocks of the total spectrum. The total application of the spectrum simulated 2340 missions of taxi, take-off, gust, maneuver, and ground-air-ground cycles. The loading frequency was 5 Hz. The total cyclic content of the spectrum consisted of 65,932 cycles.

Data Reduction and Analysis

The data taken included Krak gage output, strain gage rosette output, temperature and humidity, fatigue-crack-growth behavior, and residual strength. Various computer algorithms were used for data analysis. The outputs of the Krak gages, strain-gage rosettes, and thermocouples were analog, and continuous recordings were taken with the computer and data-storage software. Data plots of the Krak gages and thermocouples were generated every 10 seconds and correlated with applied cycles. The output of the load cells for applied loadings were continuously recorded on a strip chart recorder to show the cyclic loading as applied to each specimen. The fatigue-crack-growth behavior is presented as crack length, a , versus cycles. The strain-gage data was taken as continuous recordings of each of the legs of the strain gage rosettes. All data were stored for analysis. The axial/longitudinal strains of each rosette were used to monitor the behavior of the panel assembly during spectrum loading fatigue crack growth testing. The strain gage data plots were generated by sampling the output every 2 seconds at 50 Hz every 10 minutes. Further reduction of the strain gage data involved determining the transverse sensitivity of the strains in the composite patches and calculation of the maximum and minimum principal strains and stresses and the maximum shear strains and stresses.

Fatigue Results and Discussion

Room Temperature Results—Series 1: The spectrum loading fatigue crack growth results of one of the panel assemblies tested at room temperature and laboratory humidity is shown in Figure 6. The fatigue cracks in all of these skins (panels) of the panel assemblies were contained under the repair patches. That is, the total fatigue loading spectrum was applied without these panels failing during fatigue cycling (see Table 3). In addition, these results showed that the fatigue crack growth rate of the cracks in these panels were slow and almost constant. This indicated that the ultrasonically bonded composite patches were effective in slowing down the fatigue crack growth rate. Load transfer from the cracked skin into the composite patches was also effective as shown in the axial or longitudinal strain gage data and the reduced maximum principal stresses and maximum shear stresses. The axial strains, reduced maximum principal stresses, and maximum shear stresses in the patches show that some patches on one side of the panel assemblies were loaded higher than others (see Figures 7 and 8). In addition, the results showed that as the fatigue cracks propagated the strain and stress levels in the patches increased. This was the expected behavior since at longer crack lengths more load is transferred from the cracked skins into the patches.

180°F Steady-State Temperature Results—Series 2: The fatigue crack growth results for one of the panel assemblies tested at a steady-state temperature of 180°F (82.2°C) and laboratory humidity is shown in Figure 9. All of these panel assemblies failed during the spectrum loading fatigue cycling. Table 3 shows the summary of the fatigue results and the longest fatigue life was series panel 3-2B which survived the entire application of the spectrum, but the cracks in the skin sheets were 1.15 and 5.40 inches, respectively. The fatigue crack growth rates of the cracks in the skins of these panels showed that the rates were steadily increasing with applied cycles. At this high applied steady-state temperature of 180°F, ultrasonically bonded repair patches were effective in picking up load transferred from the cracked skins. The axial strains, the reduced maximum principal stresses, and maximum shear stresses in the patches show that some of the patches on one side of the panel assemblies were loaded higher than others.

-65°F Steady-State Temperature Results—Series 3: The spectrum loading fatigue crack growth results of one of the panel assemblies tested at -65°F and laboratory humidity is shown in Figure 10. The fatigue cracks in the skins of these panel assemblies showed a steadily increasing fatigue crack growth rate with the exception of skin sheet no. 31 which did not show much growth. The spectrum loading cyclic fatigue lives of these panel assemblies are also summarized in Table 3 and show much lower fatigue lives than the panel assemblies tested at room temperature or 180°F. The general trend of the effects of lower temperatures on structural adhesives is that the adhesive becomes more brittle at the reduced temperature of -65 F. Likewise at elevated temperatures the adhesive becomes more ductile. In both temperature cases, the ability of the composite patches to pick up load transferred from the cracked skins will be different due to the temperature effects on shear strength of the adhesive.

Prior Exposure and Room Temperature Results—Series 4: The spectrum loading fatigue crack growth results of one of the panel assemblies that were exposed for 60 days at 180°F and 95 percent RH and then room temperature tested is shown in Figure 11. The fatigue cracks in all of these skins (panels) showed a steadily increasing rate of crack growth. The fatigue cracks in skins 4,

9, and 10 were contained more than the others. The results of these panel tests summarized in Table 3 show that the spectrum loading fatigue lives were about the same as the -65°F fatigue lives, but not nearly as long as the 180°F fatigue lives. The 60-day exposure of the panels to the high temperature and humidity produced some degradation of the ultrasonically bonded patches. The mechanism is believed to be moisture diffusion into the bond lines between the patches and the aluminum skins. Degradation of the patches also occurred, since the color on some of the patches changed from black to light brown during exposure.

CONCLUSIONS

Based on the results of this experimental investigation, the following conclusions are made:

- (1) It has been successfully demonstrated that ultrasonic energy can be used to cure FM-73 structural adhesive to bond a B/E_p patch to 7075-T and T651 aluminum. The bonding time is about an hour to achieve optimum cure of the adhesive.
- (2) The ultrasonic intensity (i.e., energy per unit time per unit area) required to fully cure FM-73 in one hour is only 25 watts/square inch, and the bond strength is comparable to and often better than thermally cured specimens.
- (3) At room temperature, none of the test panels with pre-cracks failed when subjected to ground-air-ground flight spectrum loading simulating 2340 missions. At extreme conditions of temperature (-65°F and 180°F) and humidity (95 percent RH), the adhesive appears to be adversely affected and some of the test panels failed before completing 2340 missions.
- (4) Other structural adhesive systems under slightly different ultrasonic cure conditions may have the potential to be an effective adhesive for extreme conditions.

ACKNOWLEDGEMENTS

The authors would like to acknowledge Mr. Leonard Wright and his staff at The Boeing Company, Defense and Space Group, Wichita, Kansas, and Mr. Al Clark of Oklahoma Air Logistics Center, Tinker Air Force Base, Oklahoma, for supporting this project.

REFERENCES

1. Rice, R., Smith, S., Rahman, S., Broek, D., et al, "Effects of Repair on Structural Integrity", Final Report to FAA Tech Center, DOT/FAA/AM-DOT-VNTSC-FAA-93-11, July 1993.

2. Baker, A.A., and Jones, R., (Editors), *Bonded Repair of Aircraft Structures*, Martinus Nijhoff Publishers, 1988.
3. Jones, R., Molent, L., Baker, A.A., and Davis, M.J., *Bonded Repair of Metallic Components: Thick Sections*, Aeronautical Research Laboratories (ARL), Melbourne, Australia, Elsevier Science Publishers, 1988.
4. Sandow, F.A., and Cannon, R.K., "Composite Repair of Cracked Aluminum Alloy Aircraft Structure", Report Number AFWAL-TR-87-3072, AFWAL/FIB, 1987.
5. Kelly, L.G., "Composite Repair of Cracked Aluminum Structure", U. S. Air Force/Wright Aeronautical Laboratories, AGARD Conference, 1986.
6. Lincoln, J.D., 1987 ASIP/ENSIP Proceedings, AFWAL-TR88-4128, Cochran, J.B., (Lockheed/Georgia), Christian, T., and Hammond, D.O., "C-141 Repair of Metal Structures by Use of Composites", 1988.
7. U. S. Air Force Logistics Command, "Composite Patches for Metallic Structures", TT-89034, August 1989.
8. Baker, A.A., "Fibre Composite Repair of Cracked Metallic Aircraft Components -- Practical and Basic Aspects", Aeronautical Research Laboratories; Butterworth & Company, Composites, Volume 18, No. 4, 1987.
9. Caruso, R.P., "Boron/Epoxy Composites for Aircraft Structural Repair", Textron Specialty Materials Report, 1991.
10. Senapati, N., Smith, S.H., and Moulder, R., "Ultrasonic Technique for Repair of Aircraft Structures with Bonded Composite Patches - Phase I - Proof of Concept", Final Report to Boeing Defense and Space Group, October 1993.
11. ASTM Standard D3164, Determining Strength of Adhesively Bonded Plastic Lap-Shear Sandwich Joints in Shear by Tension Loading, 1993.
12. "OMEGA Complete Temperature Measurement Handbook and Encyclopedia," Volume 26, 1988.
13. ASTM D-618, "Method for Conditioning Plastics and Electrical Insulating Materials for Testing," ASTM Vol.8.01, 1993.
14. Instruction Manual, "Fractomat and Krak-Gage," Technical Bulletin KG-581 R, TTI Division, Hartrun Corporation, Chaska, Minnesota, 1982.
16. General Structural Testing of Composites, Applications Note, "Strain Gage Applications on Composites," Measurements Group, Inc., January 1988.
17. "Manual on Experimental Methods for Mechanical Testing of Composites," Edited by R. L. Pendelton and M. E. Tuttle, Society for Experimental Mechanics Inc., 1989

Table 1. The Lap Shear Strength of Ultrasonically Cured Specimens with 0.25-Inch-Thick 7075-T651 Aluminum Substrate

| Cure Condition | | | Shear Strength |
|----------------|---------------|------------|----------------|
| Power, watts | Time, minutes | B/E, plies | psi |
| 75 | 60 | 5 | 257 |
| 85 | 60 | 5 | 1,304 |
| 95 | 60 | 5 | 1,275 |
| 85 | 60 | 15 | 808 |
| 95 | 60 | 15 | 1,168 |
| 105 | 60 | 15 | 1,439 |

Table 2. Flight-by-Flight and Mission Mix Spectrum

| <p><u>MISSION A</u></p> <table border="1"> <thead> <tr> <th>f_{MAX} (KSI)</th> <th>f_{MIN} (KSI)</th> <th>CYCLES</th> </tr> </thead> <tbody> <tr> <td>22.55</td> <td>19.05</td> <td>23</td> </tr> <tr> <td>12.078</td> <td>-17.83</td> <td>1</td> </tr> <tr> <td>12.078</td> <td>9.58</td> <td>4</td> </tr> </tbody> </table> <p>1/10 FLTS f_{MAX} = 22.99</p> | | | f _{MAX} (KSI) | f _{MIN} (KSI) | CYCLES | 22.55 | 19.05 | 23 | 12.078 | -17.83 | 1 | 12.078 | 9.58 | 4 | <p><u>MISSION B</u></p> <table border="1"> <thead> <tr> <th>f_{MAX} (KSI)</th> <th>f_{MIN} (KSI)</th> <th>CYCLES</th> </tr> </thead> <tbody> <tr> <td>22.55</td> <td>19.05</td> <td>23</td> </tr> <tr> <td>17.88</td> <td>-17.86</td> <td>1</td> </tr> <tr> <td>17.88</td> <td>13.38</td> <td>9</td> </tr> </tbody> </table> <p>1/10 FLTS f_{MAX} = 22.99</p> | | | f _{MAX} (KSI) | f _{MIN} (KSI) | CYCLES | 22.55 | 19.05 | 23 | 17.88 | -17.86 | 1 | 17.88 | 13.38 | 9 |
|--|------------------------|--------|------------------------|------------------------|--------|-------|-------|----|--------|--------|---|--------|------|---|---|--|--|------------------------|------------------------|--------|-------|-------|----|-------|--------|---|-------|-------|---|
| f _{MAX} (KSI) | f _{MIN} (KSI) | CYCLES | | | | | | | | | | | | | | | | | | | | | | | | | | | |
| 22.55 | 19.05 | 23 | | | | | | | | | | | | | | | | | | | | | | | | | | | |
| 12.078 | -17.83 | 1 | | | | | | | | | | | | | | | | | | | | | | | | | | | |
| 12.078 | 9.58 | 4 | | | | | | | | | | | | | | | | | | | | | | | | | | | |
| f _{MAX} (KSI) | f _{MIN} (KSI) | CYCLES | | | | | | | | | | | | | | | | | | | | | | | | | | | |
| 22.55 | 19.05 | 23 | | | | | | | | | | | | | | | | | | | | | | | | | | | |
| 17.88 | -17.86 | 1 | | | | | | | | | | | | | | | | | | | | | | | | | | | |
| 17.88 | 13.38 | 9 | | | | | | | | | | | | | | | | | | | | | | | | | | | |
| <p><u>MISSION C</u></p> <table border="1"> <thead> <tr> <th>f_{MAX} (KSI)</th> <th>f_{MIN} (KSI)</th> <th>CYCLES</th> </tr> </thead> <tbody> <tr> <td>18.90</td> <td>16.47</td> <td>9</td> </tr> <tr> <td>9.15</td> <td>-15.25</td> <td>1</td> </tr> <tr> <td>9.15</td> <td>6.65</td> <td>1</td> </tr> </tbody> </table> <p>1/10 FLTS f_{MAX} = 19.29</p> | | | f _{MAX} (KSI) | f _{MIN} (KSI) | CYCLES | 18.90 | 16.47 | 9 | 9.15 | -15.25 | 1 | 9.15 | 6.65 | 1 | <p><u>MISSION D</u></p> <table border="1"> <thead> <tr> <th>f_{MAX} (KSI)</th> <th>f_{MIN} (KSI)</th> <th>CYCLES</th> </tr> </thead> <tbody> <tr> <td>18.97</td> <td>16.47</td> <td>10</td> </tr> <tr> <td>9.15</td> <td>-11.47</td> <td>1</td> </tr> <tr> <td>9.15</td> <td>6.65</td> <td>1</td> </tr> </tbody> </table> <p>1/10 FLTS f_{MAX} = 19.29</p> | | | f _{MAX} (KSI) | f _{MIN} (KSI) | CYCLES | 18.97 | 16.47 | 10 | 9.15 | -11.47 | 1 | 9.15 | 6.65 | 1 |
| f _{MAX} (KSI) | f _{MIN} (KSI) | CYCLES | | | | | | | | | | | | | | | | | | | | | | | | | | | |
| 18.90 | 16.47 | 9 | | | | | | | | | | | | | | | | | | | | | | | | | | | |
| 9.15 | -15.25 | 1 | | | | | | | | | | | | | | | | | | | | | | | | | | | |
| 9.15 | 6.65 | 1 | | | | | | | | | | | | | | | | | | | | | | | | | | | |
| f _{MAX} (KSI) | f _{MIN} (KSI) | CYCLES | | | | | | | | | | | | | | | | | | | | | | | | | | | |
| 18.97 | 16.47 | 10 | | | | | | | | | | | | | | | | | | | | | | | | | | | |
| 9.15 | -11.47 | 1 | | | | | | | | | | | | | | | | | | | | | | | | | | | |
| 9.15 | 6.65 | 1 | | | | | | | | | | | | | | | | | | | | | | | | | | | |
| <p><u>MISSION E</u></p> <table border="1"> <thead> <tr> <th>f_{MAX} (KSI)</th> <th>f_{MIN} (KSI)</th> <th>CYCLES</th> </tr> </thead> <tbody> <tr> <td>22.55</td> <td>19.05</td> <td>23</td> </tr> <tr> <td>10.14</td> <td>-18.59</td> <td>1</td> </tr> <tr> <td>10.14</td> <td>7.64</td> <td>1</td> </tr> </tbody> </table> <p>1/10 FLTS f_{MAX} = 22.99</p> | | | f _{MAX} (KSI) | f _{MIN} (KSI) | CYCLES | 22.55 | 19.05 | 23 | 10.14 | -18.59 | 1 | 10.14 | 7.64 | 1 | <p><u>MISSION F*</u></p> <table border="1"> <thead> <tr> <th>f_{MAX} (KSI)</th> <th>f_{MIN} (KSI)</th> <th>CYCLES</th> </tr> </thead> <tbody> <tr> <td>23.80</td> <td>14.30</td> <td>50</td> </tr> </tbody> </table> | | | f _{MAX} (KSI) | f _{MIN} (KSI) | CYCLES | 23.80 | 14.30 | 50 | | | | | | |
| f _{MAX} (KSI) | f _{MIN} (KSI) | CYCLES | | | | | | | | | | | | | | | | | | | | | | | | | | | |
| 22.55 | 19.05 | 23 | | | | | | | | | | | | | | | | | | | | | | | | | | | |
| 10.14 | -18.59 | 1 | | | | | | | | | | | | | | | | | | | | | | | | | | | |
| 10.14 | 7.64 | 1 | | | | | | | | | | | | | | | | | | | | | | | | | | | |
| f _{MAX} (KSI) | f _{MIN} (KSI) | CYCLES | | | | | | | | | | | | | | | | | | | | | | | | | | | |
| 23.80 | 14.30 | 50 | | | | | | | | | | | | | | | | | | | | | | | | | | | |
| <p><u>TEST MISSION MIX</u></p> <p>BLOCK 1 = ABCABDEFABCAB BLOCK 2 = BEFBECBEFBECA</p> <p>REPEAT MIX = 5(BLOCK 1) + (BLOCK 2)</p> <p>NOTE: SPECTRA FOR B-52G/H WING UPPER SURFACE AT W.S. 402, S-21 MISSION MIX FOR B-52G/H BASELINE II AIR CREW CONTINUATION TRAINING USAGE</p> | | | | | | | | | | | | | | | | | | | | | | | | | | | | | |

Table 3. Summary of Fatigue Life Results for All Panel Assemblies Tested

| Panel Assembly Test Series | Testing Environment | Total Applied Fatigue Cycles of Spectrum | Comments |
|----------------------------|-----------------------|--|--------------|
| 3-1A | Room temperature | 65,932 | Did not fail |
| 3-1B | Room temperature | 63,373 | Did not fail |
| 3-1C | Room temperature | 65,932 | Did not fail |
| 3-2A | 180°F | 40,937 | Failure |
| 3-2B | 180°F | 65,931 | Failure |
| 3-2C | 180°F | 47,778 | Failure |
| 3-3A | -65°F | 17,463 | Failure |
| 3-3B | -65°F | 20,747 | Failure |
| 3-3C | -65°F | 24,024 | Failure |
| 3-4A | Room temperature | 19,231 | Failure |
| 3-4B | following exposure at | 25,563 | Failure |
| 3-4C | 180°F and 96% RH | 20,313 | Failure |

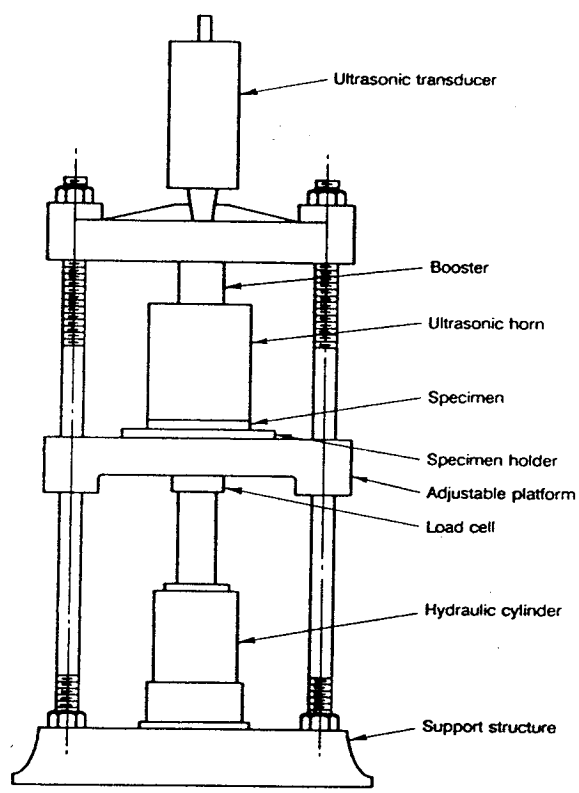


Figure 1. Schematic experimental setup for ultrasonic activation of adhesives.

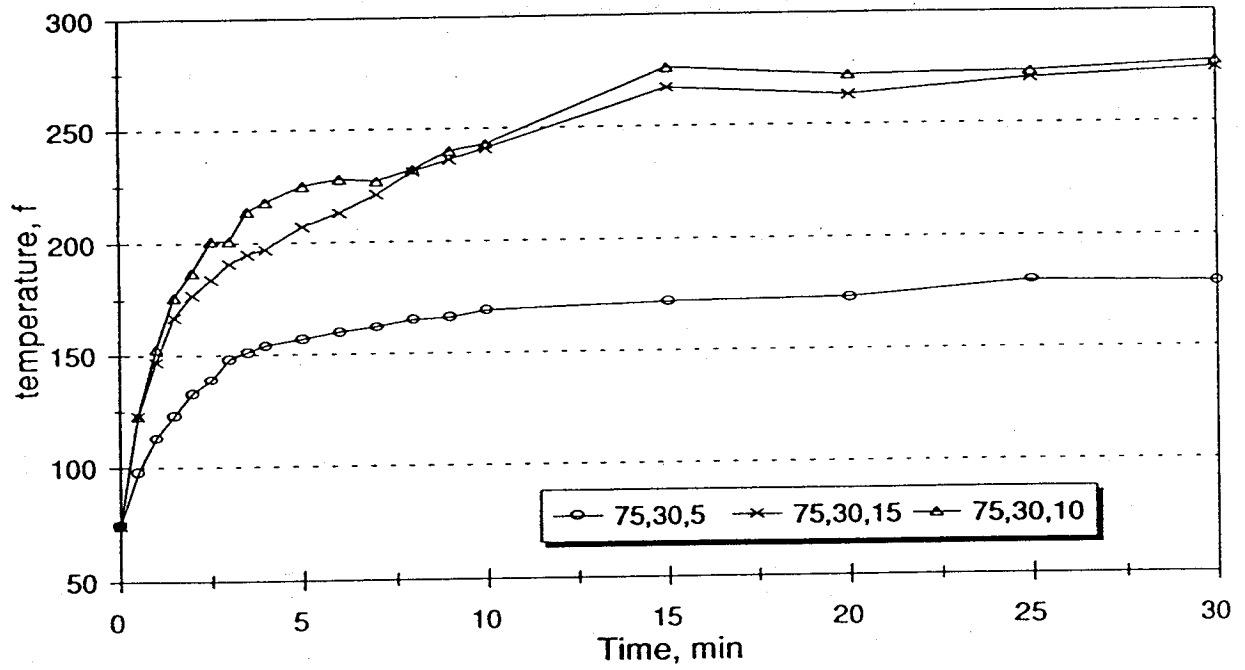


Figure 2. Plot of temperature versus time for three variable combinations.

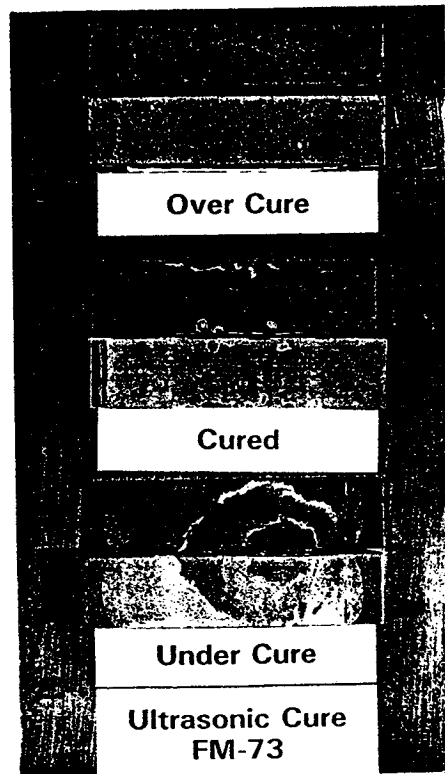


Figure 3. Baseline specimens for degree of cure evaluation.

Some original figures were unavailable at publication.)

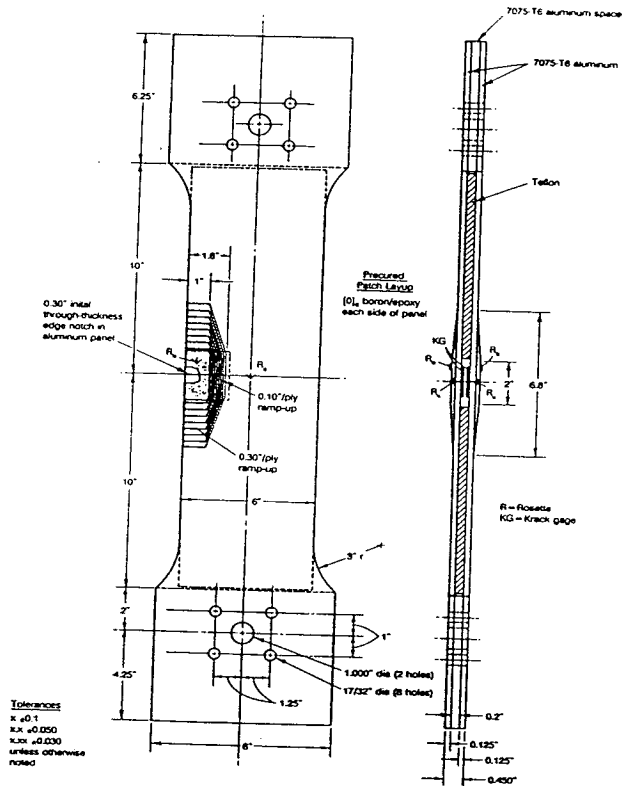
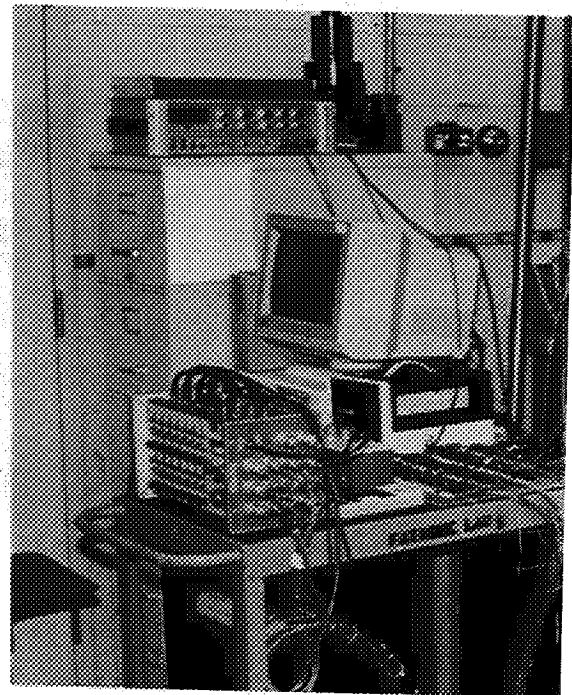
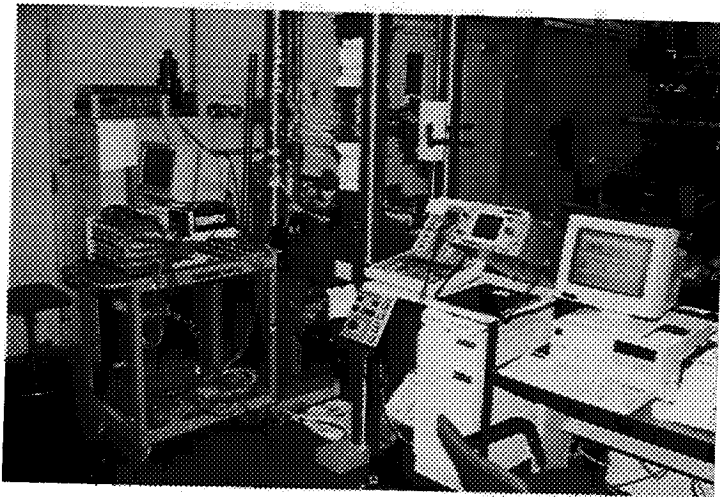


Figure 4. Simulated repair specimen with edge crack - instrumentation. (R = Rosette, KG = KRAK-GAGE).



(a) Testing setup and instrumentation.

(b) Strain and Krak gage instrumentation.

Figure 5. Instron 50 Kip electrohydraulic testing machine for fatigue and residual strength testing of repaired panels.

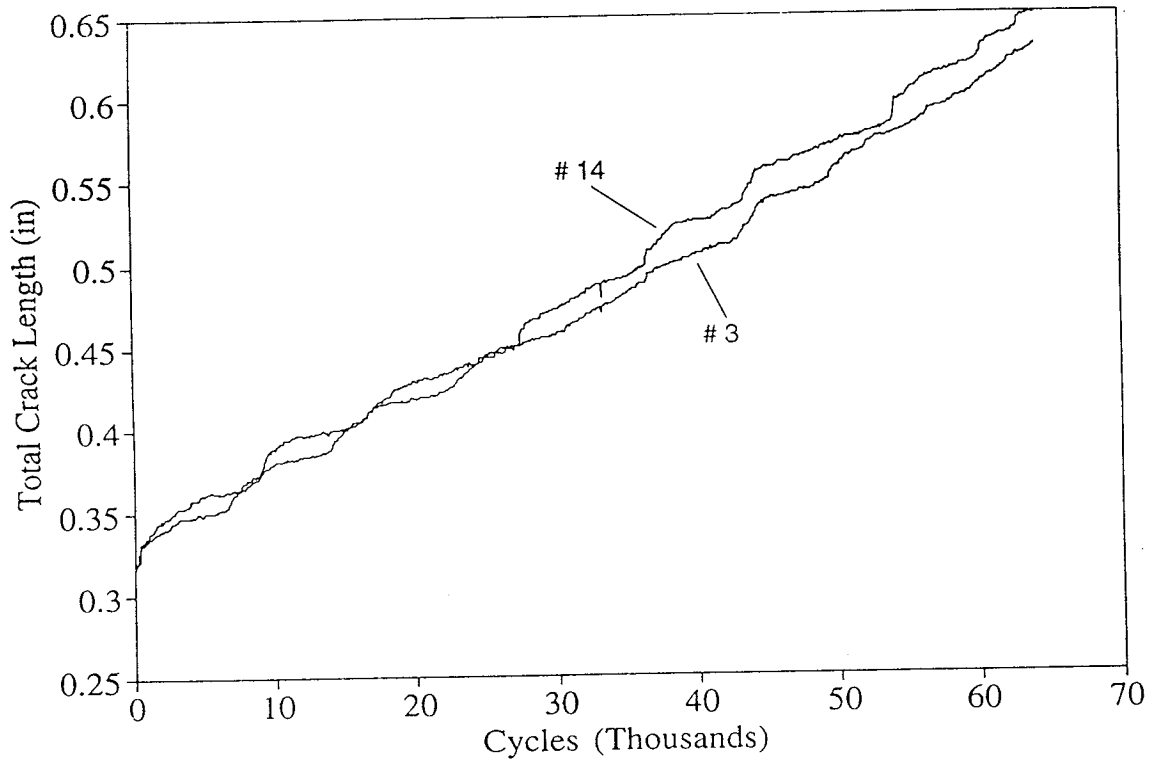


Figure 6. Spectrum loading fatigue crack growth results for skins (panels) 3 and 14, panel assembly 3-1A, room temperature.

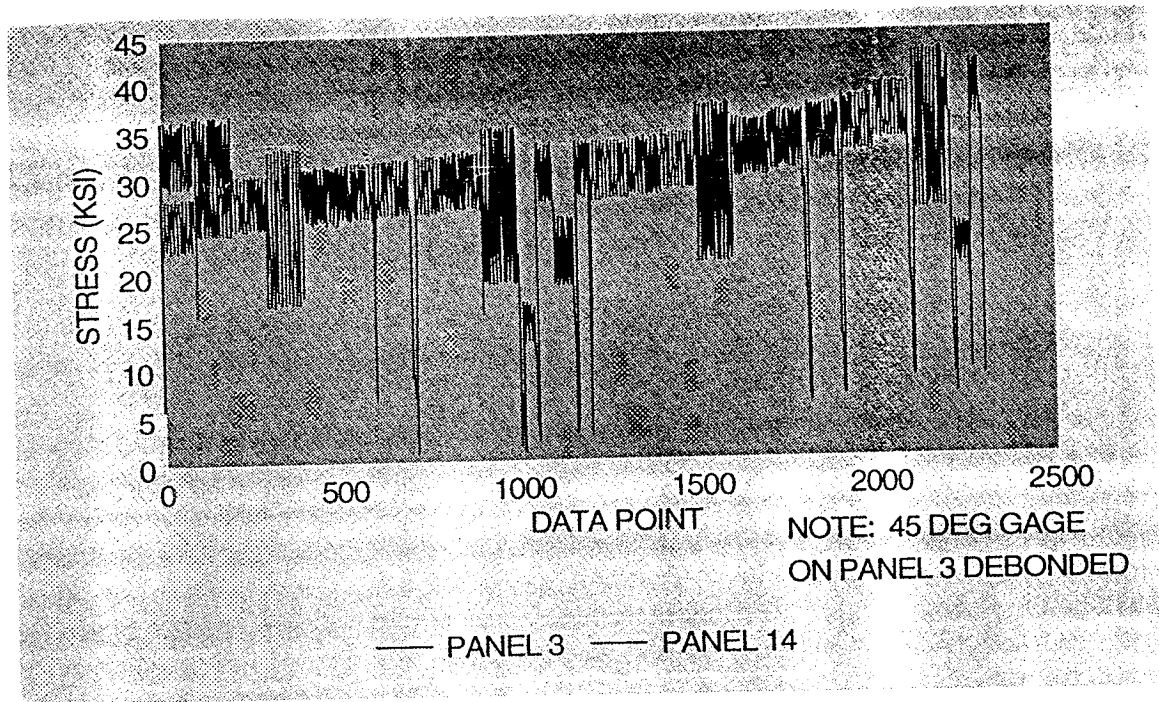


Figure 7. Maximum principal stresses in aluminum skins (panels) 3 and 14, panel assembly 3-1A, room temperature.

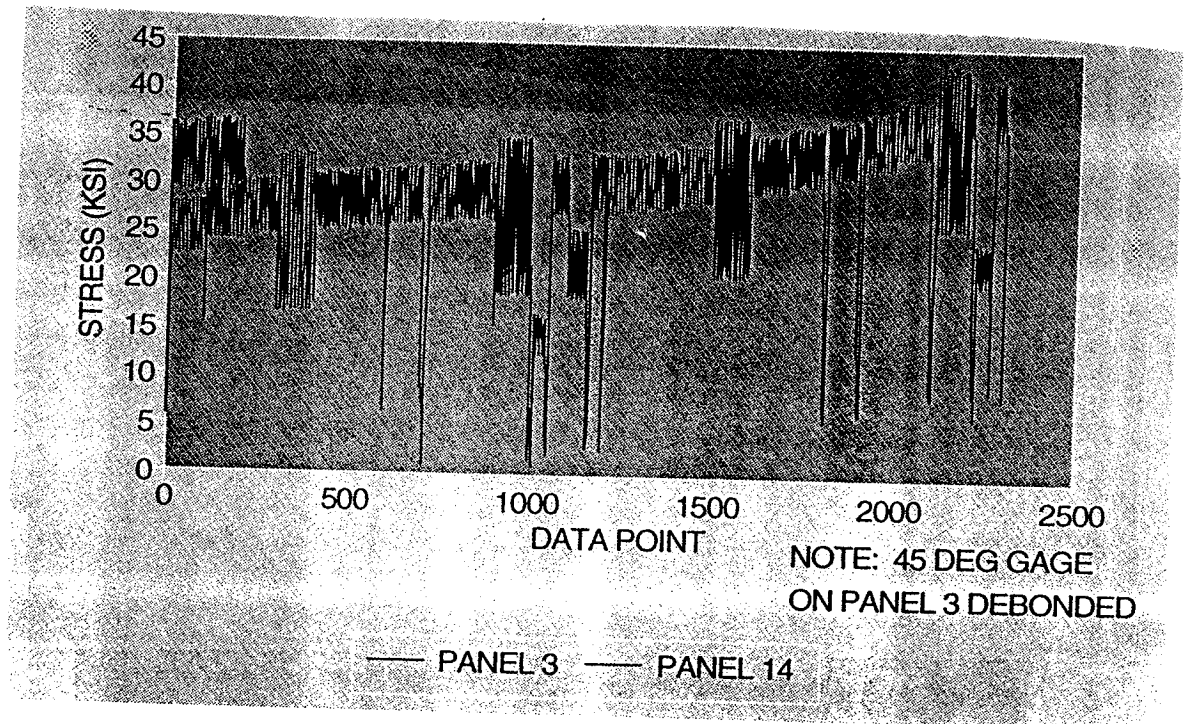


Figure 8. Maximum principal stresses in boron/epoxy patches on skins (panels) 3 and 14, panel assembly 3-1A, room temperature.

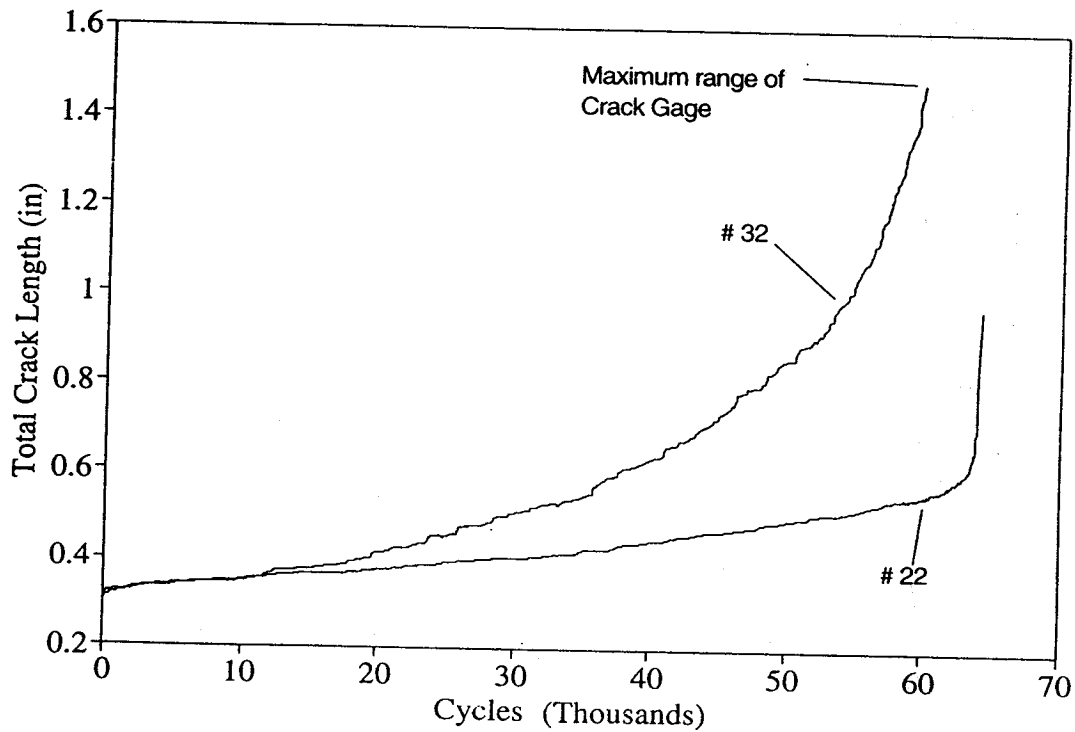


Figure 9. Spectrum loading fatigue crack growth results for skins (panels) 22 and 32, panel assembly 3-2B, 180°F temperature.

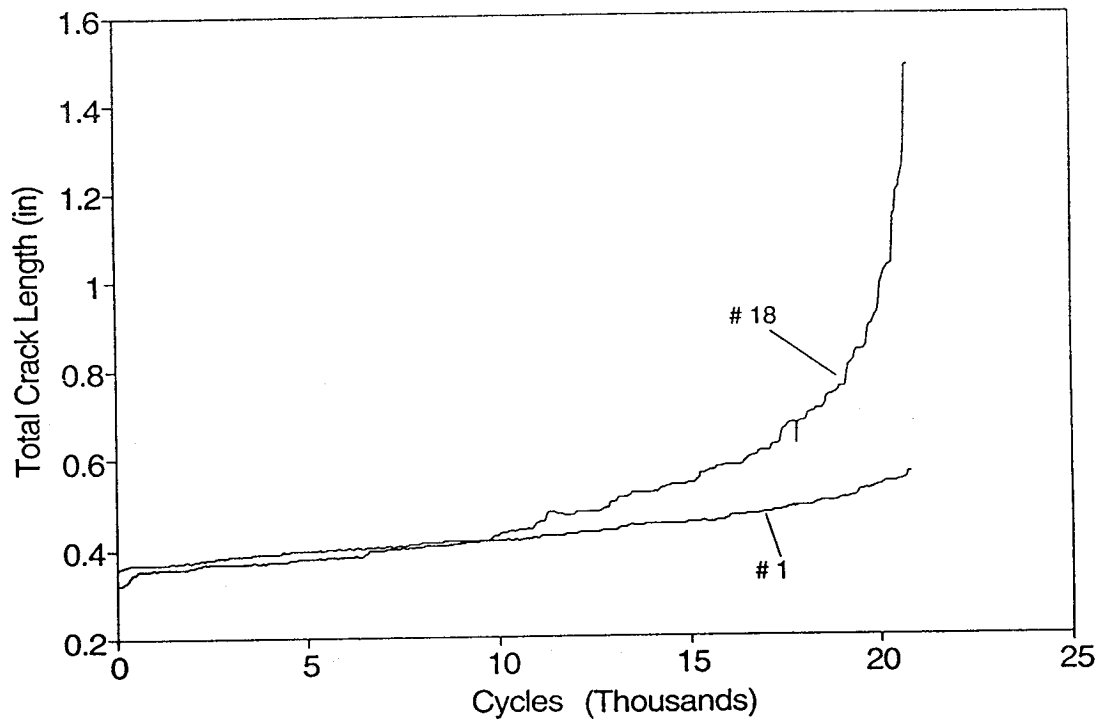


Figure 10. Spectrum loading fatigue crack growth results for skins (panels) 1 and 18, panel assembly 3-3B, -65°F temperature.

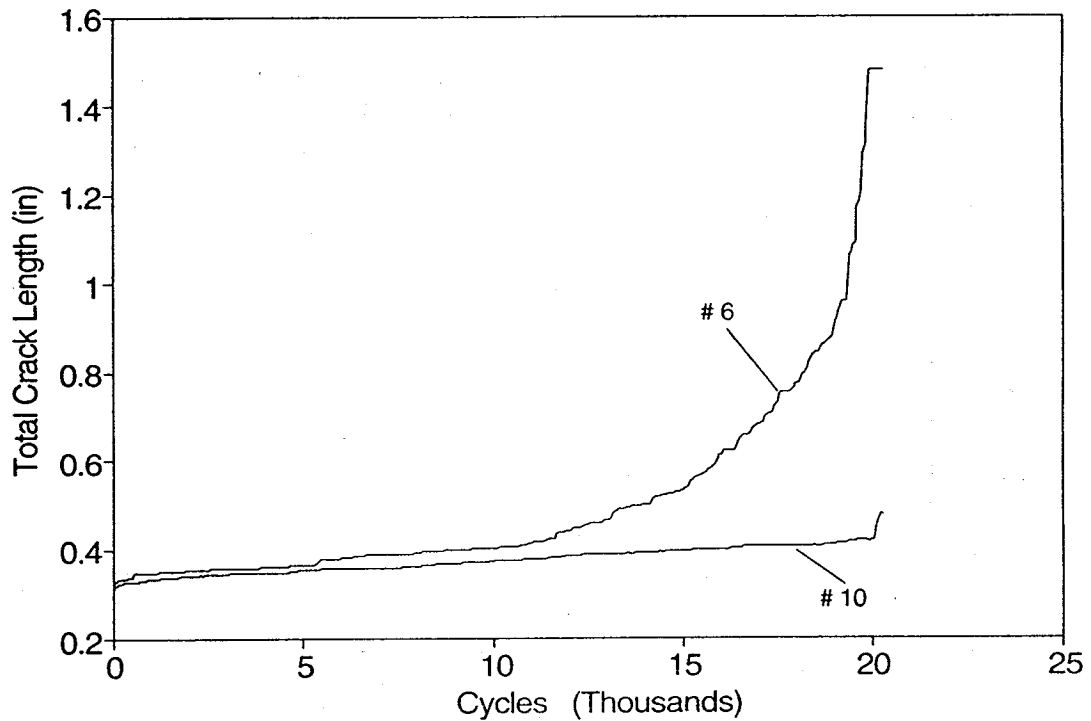


Figure 11. Spectrum loading fatigue crack growth results for skins (panels) 6 and 10, panel assembly 3-4C, prior exposure and room temperature.